INFECTION AND IMMUNITY, Apr. 2007, p. 1577–1585 Vol. 75, No. 4
0019-9567/07/$08.00+0 doi:10.1128/IAI.01392-06

Solitary Intestinal Lymphoid Tissue Provides a Productive Port of Entry for *Salmonella enterica* Serovar Typhimurium▽

Stephan Halle,[1] Dirk Bumann,[2] Heike Herbrand,[1] Yvonne Willer,[2] Sabrina Dähne,[1] Reinhold Förster,[1] and Oliver Pabst[1]*

Institute of Immunology, Hannover Medical School, 30625 Hannover, Germany,[1] and Junior Research Group "Mucosal Infections," Institute of Immunology, Hannover Medical School, 30625 Hannover, Germany[2]

Received 30 August 2006/Returned for modification 20 November 2006/Accepted 22 January 2007

Oral infection of mice with *Salmonella enterica* serovar Typhimurium results in the colonization of Peyer's patches, triggering a vigorous inflammatory response and immunopathology at these sites. Here we demonstrate that in parallel to Peyer's patches a strong inflammatory response occurs in the intestine, resulting in the appearance of numerous inflammatory foci in the intestinal mucosa. These foci surround small lymphoid cell clusters termed solitary intestinal lymphoid tissue (SILT). *Salmonella* can be observed inside SILT at early stages of infection, and the number of infected structures matches the number of inflammatory foci arising at later time points. Infection leads to enlargement and morphological destruction of SILT but does not trigger de novo formation of lymphoid tissue. In conclusion, SILT, a lymphoid compartment mostly neglected in earlier studies, represents a major site for *Salmonella* invasion and ensuing mucosal pathology.

Although the epithelia lining the intestine provide a tight barrier against potentially harmful antigens and microbes, homeostasis of intestinal immune functions requires monitoring of the intestinal microflora. This is achieved by a controlled uptake of luminal microbiota into mucosal tissues by specialized microfold (M) cells and lamina propria dendritic cells (11, 20). This gateway into the host is exploited by various enteropathogens such as *Salmonella*, *Yersinia*, and *Shigella* spp. These bacteria express genes that allow them to adhere to and invade M cells and thereby infect host tissues (7, 14, 26). It is well known that M cells are present in the follicle-associated epithelium (FAE) overlying Peyer's patches (PP) (19), and consequently PP are considered to represent important mediators of mucosal pathogenicity displayed by these bacteria.

However, M cells are also sporadically present in morphologically inconspicuous villi (intravillus M cells) (12). Although the frequency of M-cell-containing villi is low, their number might increase upon stimulation, and intravillus M cells have been suggested to support *Salmonella* invasion in lymphotoxin α mutants which lack any organized lymphoid tissue in the intestine (12). Another gateway into the organism might be provided by dendritic cells residing in the intestinal lamina propria. These cells have been shown to extend dendrites through the epithelial lining into the intestinal lumen, which might allow such cells to directly sample antigens as well as pathogens (21, 27, 28). Indeed, there is solid evidence showing that the ability to target M cells and colonize PP is not mandatory for the development of systemic disease caused by *Salmonella enterica*. Vasquez-Torrez et al. demonstrated that salmonellae that are unable to target M cells can penetrate the intestinal barrier and disseminate in a β2-integrin-dependent mechanism (34). Similarly, *Yersinia enterocolitica* utilizes invasin-dependent and invasin-independent routes for systemic dissemination (9). Furthermore, hepatosplenic infection by *Yersinia pseudotuberculosis* has been suggested to be independent of prior colonization of lymphoid organs, but to result from direct dissemination of bacteria replicating in the intestinal lumen into the circulation (2).

Despite these alternative infection pathways that appear to contribute to the systemic dissemination of *Salmonella*, M-cell penetration, along with the subsequent infection of the underlying lymphoid tissue, is considered the main route of *Salmonella* infection of the intestinal mucosa (29). Besides PP, M cells have been described in the FAE of small lymphoid aggregations, termed isolated lymphoid follicles (ILF), that exist in the small intestine of numerous species, including mice and humans (8, 18, 24). ILF share many architectural features with PP, including a compact B-cell rich follicle covered by the subepithelial dome region consisting of dendritic cells and an overlying FAE including M cells. Consistent with such architectural features, ILF are capable of supporting immunoglobulin production in response to *Salmonella* infection (16), as well as to oral immunization (35). We have recently suggested that ILF do not constitute a separate type of lymphoid organ but merely represent a particularly well-organized manifestation of a common lymphoid structure that we termed solitary intestinal lymphoid tissue (SILT) (24). The entire spectrum of SILTs ranges from small lymphoid aggregations mostly filled with stem cell-like cells, also referred to as cryptopatches (CP), to larger ILF that resemble a single dome of PP. SILT structures are interconvertible; thus, CP can develop into ILF, and ILF might revert into CP (see Fig. 2E). Conversion of small SILT into fully developed SILT can be triggered by external influences, including microbial stimulation (23). Consequently, the spectrum of SILTs observed in germfree mice is predominated by particularly small structures resembling CP, whereas ILF are absent in such mice. In response to microbial colonization of germfree mice, the spectrum of SILTs adapts to

* Corresponding author. Mailing address: Institute of Immunology, Hannover Medical School, Carl-Neuberg Strasse 1, 30625 Hannover, Germany. Phone: 49-511-5329725. Fax: 49-511-5329722. E-mail: Pabst.Oliver@mh-hannover.de.

▽ Published ahead of print on 5 February 2007.

encompass a broad spectrum of differently sized structures, now including ILF (23). Thus, the entire array of differently organized SILT structures is subject to environmental influences and will frequently contain numerous SILTs that display intermediate phenotypes between CP and ILF. In contrast to its dynamic phenotype, the frequency of SILTs invariantly ranges from 40 to 60 structures per square centimeter throughout the murine small intestine, resulting in more than 1,000 SILT structures in the intestine (24). Thus, usually the overall number of SILTs by far exceeds that of ILF. Consequently, SILT provides a prominent source of M cells and might substantially contribute to invasion of pathogens with M-cell tropism.

We report here that SILT can be targeted by *Salmonella* for tissue entry, causing a local inflammation and immunopathology in these structures. Quantification of inflammatory foci in the intestinal mucosa suggests that, in addition to PP, SILT substantially contributes to *Salmonella*-induced mucosal pathology.

MATERIALS AND METHODS

Preparation of sections and microscopy. C57BL/6 and BALB/c mice were bred at the central animal facility of Hannover Medical School under specific-pathogen-free conditions or purchased from Charles River (Germany). Adult mice were sacrificed by CO_2 inhalation. The small intestine was excised, flushed with phosphate-buffered saline (PBS), and opened along the mesenteric side. For horizontal sections fragments about 20 mm in length were flattened with the mucosal side downward on filter paper, embedded in OCT compound, and frozen on dry ice. For vertical sections gut fragments approximately 5 cm in length were washed in PBS, followed by a 50% mixture of OCT and PBS, and transferred to OCT before Swiss rolls with the luminal side facing outward and the proximal end located at the center of the roll were prepared. Cryosections (8 μm) were air dried and fixed for 10 min in ice-cold acetone.

***Salmonella* infections.** All *Salmonella* strains used in the present study were derivatives of *S. enterica* serovar Typhimurium strain SL1344 (10). Mutations were introduced by using red recombinase-mediated homologous recombination (5) with the primers described at http://falkow.stanford.edu/whatwedo/wanner/. First, we exchanged the *aroA* gene against a kanamycin resistance cassette that was subsequently cured by recombination using plasmid pCP20 as described previously (5). Unless indicated otherwise, all experiments were performed with this strain. For the experiments shown in Fig. 3A the double mutants SL1344 *aroA sipB* and SL1344 *aroA ssrB* were also used. The kanamycin resistance cassette in *sipB* was again cured to avoid polar effects on the expression of downstream genes. For detection of live *Salmonella* in tissues (see Fig. 3C), a red fluorescent variant was generated. SL1344 *aroA* was engineered to carry plasmid pDsRed in which a bright DsRed variant (32), which was destabilized by fusing a recognition site for the tail-specific protease to its C terminus (1), was expressed from the P_{pagC} promoter. *Salmonella* strains were grown in LB broth containing 90 μg of streptomycin/ml and either 100 μg of ampicillin/ml or 30 μg of kanamycin/ml when appropriate. For oral infection *Salmonella* strains were grown to a density of 10^8 bacteria/ml. Bacteria were washed twice with LB broth and resuspended at 10^8 bacteria in 200 μl of LB broth containing 3% $NaHCO_3$. Mice had free access to water and food and were inoculated orally with 200 μl of suspension with a feeding needle. The number of inoculated bacteria and of salmonellae present in tissues was determined by plating. The PP and mesenteric lymph nodes were disrupted as described for flow cytometry. In order to determine the number of salmonellae in non-PP-bearing intestines, intestinal tubes were vigorously washed with PBS containing 50 μg of gentamicin/ml, followed by PBS alone, and homogenized by using an Ultra Turrax. Triton X-100 was added to a final concentration of 0.1%, and tissue suspensions were vortexed for 30 s before plating serial dilutions.

Antibodies. The following antibodies and conjugates were used in the present study: anti-CD11b-fluorescein isothiocyanate (FITC; Caltag), anti-CD11c-bio, anti-GR1-phycoerythrin, anti-L6G-FITC, anti-Ly6G-bio (BD Biosciences), anti-CD117 (cKit, clone ACK2; Natutec) and anti-B220 (clone TIB146, provided by Elisabeth Kremmer, GSF München). Cy5 conjugate of anti-B220 was prepared as recommended by the manufacturer (Amersham). Biotinylated antibodies were recognized by streptavidin-coupled to Alexa488, Cy3, or Cy5 (Molecular Probes). Unconjugated anti-cKit was recognized by mouse anti-rat-Cy3 conjugate (Jackson Laboratories). Salmonellae were detected using a polyclonal anti-*Salmonella* serum raised in rabbits (SIFIN, Germany), followed by goat anti-rabbit-FITC conjugate (Jackson Laboratories).

Immunohistochemistry. Sections were rehydrated in TBS (0.1 M Tris [pH 7.5], 0.15 M NaCl) supplemented with 0.1% Tween 20 (TBST) and transferred into a vertical flow staining chamber (Thermo Life Sciences). Sections were preincubated twice with TBST containing 5% rat or mouse serum, depending on the antibodies to be used. Sections were incubated with a mixture of appropriately diluted biotinylated or fluorescent dye-coupled antibodies in 2.5% serum–TBST for 1.5 h and washed three times with TBST. If required sections were subsequently incubated with a streptavidin conjugate in 2.5% serum in TBST for 1 h. Sections were washed three times with TBST and stained twice for 2 min with 1 μg of DAPI-TBST/ml to visualize nuclei. Sections were washed three times with TBST and mounted with Mowiol. Staining with unconjugated antibodies (anti-*Salmonella* and anti-cKit) was performed for 45 min in TBST containing 2.5% mouse serum, followed by detection with Cy3- or FITC-conjugated secondary reagents (mouse anti-rat-Cy3 or goat anti-rabbit-FITC). For analysis of the distribution and cellular composition of lymphoid aggregations, composite images were automatically assembled by using a motorized Axiovert 200M microscope (Carl Zeiss) with autofocus module Axiovision 4.0 software (Carl Zeiss).

Flow cytometry. To obtain single cell suspensions of mesenteric lymph nodes and PP, organs were minced between two rough glass slides and washed with PBS supplemented with 2% fetal calf serum (FCS). For isolation of cells from the lamina propria, gut content and PP were removed before the intestines were opened longitudinally. Intestines were washed twice in cold PBS and incubated for 10 min in 10 ml of Hanks balanced salt solution supplemented with 10% FCS and 2 mM EDTA at 37°C in a water bath. Subsequently, the tubes were shaken vigorously for 10 s, and the supernatant containing epithelial cells was discarded. This incubation was repeated twice, the remaining tissue washed in PBS and incubated at 37°C for 45 min in RPMI with 20% FCS and 0.5 mg of collagenase A (Roche)/ml. Cells were liberated from the digested tissue by shaking the tubes for 10 s, and the supernatants were filtered through a nylon mesh. After centrifugation the cell pellet was resuspended in isotonic 40% Percoll (Amersham) in RPMI with 5% FCS. This cell suspension was overlaid onto 70% Percoll in RPMI with 5% FCS and centrifuged at $800 \times g$ for 20 min. Cells were recovered from the interphase, washed twice in PBS with 2% FCS, and stained using the antibodies described above.

Statistical analysis. Statistical analysis was performed by using GraphPad Prism 4.0 software and applying anonparametric two-tailed Mann-Whitney test. Statistical differences are indicated as follows: ns, not significant; ***, $P < 0.001$.

RESULTS

***Salmonella* infection results in mucosal inflammation in and outside PP.** M cells present in the epithelium overlying PP are well known to be targeted by different enteropathogens, thereby enabling their uptake into the intestinal mucosa (7, 14, 26). In addition, alternative routes of entry via M cells outside of PP (12, 16), via lamina propria dendritic cells (21, 27), or by direct invasion of absorptive enterocytes have been proposed. However, the relevance of these different mechanisms for *Salmonella* mucosal pathogenicity has not yet been explored. In order to quantitatively compare PP-dependent and -independent routes of mucosal infection, BALB/c and C57BL/6 mice were infected orally with an attenuated *aroA*-deficient *S. enterica* serotype Typhimurium strain (see Materials and Methods). This strain does not cause fatal disease and thus allows analysis at late stages of infection. Mice were sacrificed 2, 5, 7, and 13 days postinfection, and the bacterial load in mesenteric lymph nodes and individual PP was determined (Fig. 1A and data not shown). *Salmonella* could be detected in all individual PP and in the mesenteric lymph nodes of both mouse strains. In agreement with previous observations, the number of salmonellae present in the PP increased until 7 days postinfection. Subsequently, it decreased until 13 days postinfection to roughly the bacterial load observed at day 2 postinfection,

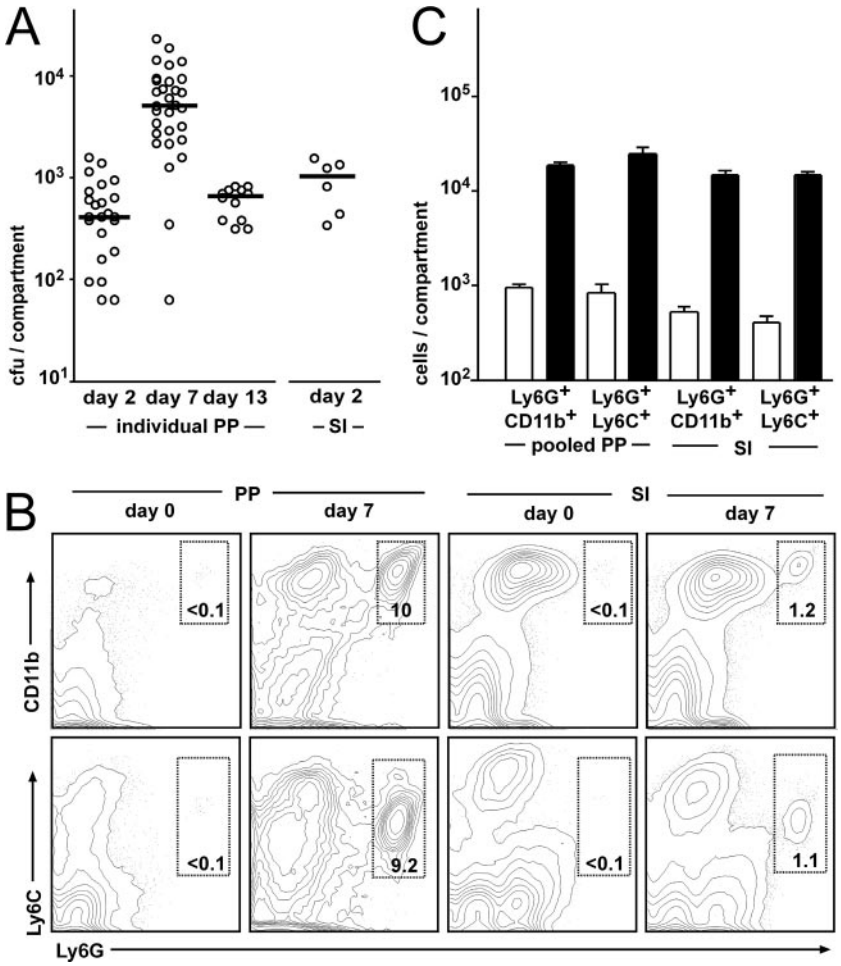

FIG. 1. Oral *Salmonella* infection results in inflammatory responses in PP and in non-PP-bearing intestines. BALB/c mice were inoculated orally with 10^8 live salmonellae. (A) On days 2, 7, and 13 postinfection the bacterial load in individual PP was determined by plating serial dilutions of disintegrated PP cell suspensions. In addition, the bacterial load in non-PP-bearing small intestinal tissue (SI) was determined on day 2 postinfection. The open circles represent the numbers of salmonellae cultivated from individual PP and the small intestine after all PP had been removed. The median is indicated by horizontal bars. (B) On day 7 postinfection the cells were isolated from pooled PP and the entire small intestinal lamina propria and analyzed by flow cytometry. Contour plots display live ($DAPI^-$) immune cells ($Ly5.2^+$) analyzed for Ly6G, CD11b, and Ly6C expression. The numbers indicate the percentages of cells in the boxed regions that display a $Ly6G^{hi}$ $Ly6C^{intermediate}$ $CD11b^{hi}$ phenotype, which is indicative for activated neutrophils. (C) Absolute cell numbers of inflammatory cells present in pooled PP and entire small intestinal lamina propria of uninfected mice (□) and 7 days postinfection (■). The results for one representative experiment of three experiments performed with four animals per group each is depicted. Bars represent the medians, and error bars indicate the standard deviations.

indicating the efficient clearance of most bacteria from the tissue. Similarly, the number of salmonellae present in the mesenteric lymph nodes increased until 7 days postinfection but, compared to the PP, declined more slowly and at day 13 postinfection the number of salmonellae was still similar to the bacterial load observed at 5 days postinfection (data not shown). Moreover, we determined the number of salmonellae present in the entire small intestine outside the PP at 2 days after infection. We observed that *Salmonella* could be cultivated from small intestinal tissue even after all the PP had been carefully removed (Fig. 1A). The number of bacteria recovered from the small intestines without PP was higher compared to the number of salmonellae cultivated from individual PP but did not reach the number of bacteria cultivated from pooled PP (Fig. 1A and data not shown). However, the recovery efficacy of *Salmonella* might depend on the amount of tissue used. In particular, plating of tissue homogenates derived from large amounts of tissue, such as the non-PP-bearing intestines, might underestimate the actual number of salmonellae.

In order to determine the degree of inflammation in the intestinal mucosa, we quantified the number of inflammatory cells present in PP and in the PP-free small intestine at the peak of infection, i.e., at 7 days postinfection, by flow cytometry. The markers used included CD45.2, which allows the identification of all immune cells in combination with $Ly6C^+$, $Ly6G^+$, and $CD11b^+$ cells, allowing the detection of neutrophils and macrophages. We observed that the number of inflammatory cells present in both the PP and the intestinal mucosa outside the PP increased dramatically after infection (Fig. 1B), thus indicating the existence of inflammatory infiltrates outside PP. Infiltrating cells were mostly $Ly6C^+$ $Ly6G^+$ $CD11b^+$ and displayed a high side-scatter profile, suggesting

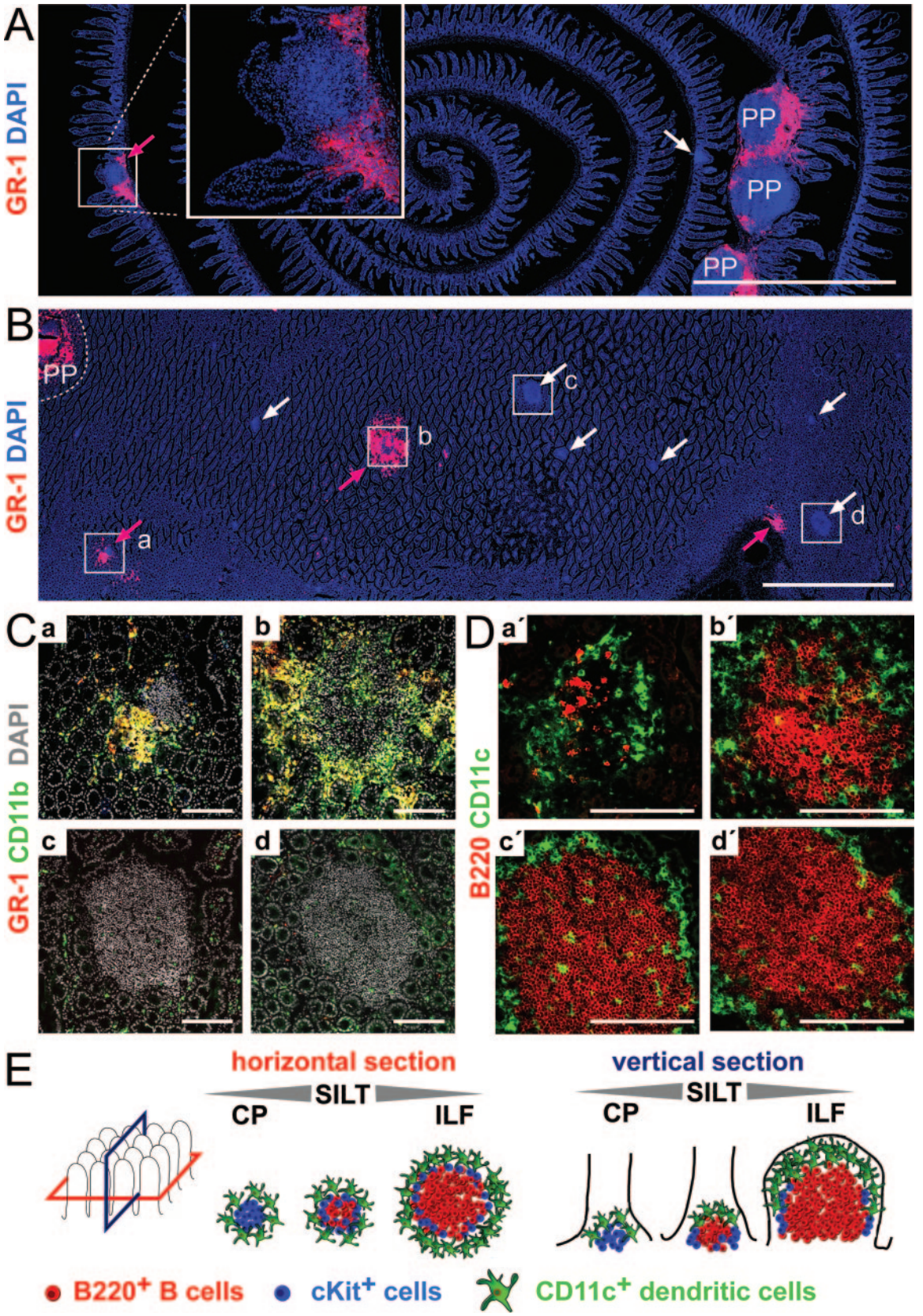

FIG. 2. Inflammatory cell infiltrates localize to PP and SILT in the intestinal mucosa. At 7 days after *Salmonella* infection the localization of inflammatory cells in the intestinal mucosa was analyzed. (A) Vertical sections through small intestinal rolls were stained for nuclei (blue) and with anti-GR-1 antibody (red), which is indicative for inflammatory cells. Overview images that allow the assessment of large coherent areas of the

that the majority of these cells were neutrophils (Fig. 1B). $CD11b^+$ cells that are constitutively present in the lamina propria (Fig. 1B) were almost exclusively $CD11c^+$, indicating that these cells are lamina propria dendritic cells (data not shown). Quantification of the absolute cell numbers of $Ly6G^+$ $CD11b^+$ and $Ly6G^+$ $Ly6C^+$ cells in uninfected BALB/c mice compared to animals at 7 days postinfection revealed that the overall number of inflammatory cells present in the infected, PP-free lamina propria was similar to that identified in all pooled PP (Fig. 1C). No major differences were observed in the frequency of inflammatory cells or the number of cultivatable *Salmonella* organisms between proximal and distal segments of the small intestine (data not shown). In conclusion, these observations indicate that a major part of the overall inflammatory response occurs outside PP.

Mucosal inflammatory foci are invariantly associated with SILT. In order to localize the inflammatory cells outside PP, we analyzed vertical and horizontal sections through the intestine 7 days after *Salmonella* infection by automated multicolor fluorescence microscopy. Vertical sections were cut along the crypt villus axis, whereas horizontal sections were cut through the "crypt zone" (see Fig. 2E for a schematic illustration of cutting planes). Sections were stained for nuclei and with an anti-GR-1 antibody, detecting the epitopes recognized by anti-Ly6C and anti-Ly6G antibodies and thereby highlighting inflammatory infiltrates. As expected, we observed massive infiltration of $GR\text{-}1^+$ cells within the PP (Fig. 2A and B). Whereas both vertical and horizontal sections (Fig. 2A and B) may be helpful in detecting inflammatory foci outside PP, the use of horizontal sections through the "crypt zone" was especially suited to systematically identify all inflammatory foci present in a given area of the intestine. By this means multiple additional foci of $GR1^+$ inflammatory cells were identified outside the PP (Fig. 2A, B, and C). This finding confirms our results obtained by flow cytometry that *Salmonella* infection results in considerable inflammation outside the PP. Such sites were scattered throughout the intestinal wall in both the proximal and the distal small intestine, and their localization was independent of the distance to the nearest-neighbor PP. No additional sites of inflammation could be detected on serial horizontal sections at the level of the villi compared to "crypt zone" sections, indicating that the method of using these horizontal sections was appropriate to record all inflammatory foci. We never observed inflammatory foci in uninfected wild-type mice, confirming that the detected mucosal inflammation is caused by *Salmonella* infection.

Inflammatory cells generally accumulated in close proximity to dense aggregations of lymphoid cells (Fig. 2A, B, and C). In order to characterize such sites in more detail, we stained serial sections with anti-B220, anti-CD11c (Fig. 2D), anti-CD3, and anti-cKit antibodies (data not shown). We observed that these structures are distinguished by a typical spatial arrangement of $CD11c^+$ cells fringing a core composed of $cKit^+$ and $B220^+$ cells and some interspersed $CD3^+$ T cells (Fig. 2D and E and data not shown). The spatial distribution, as well as the cellular composition and architecture of the accompanying aggregates, identifies these sites as SILT (see above and Fig. 2E). Notably, inflammatory infiltrates could be observed in SILTs displaying a broad spectrum of phenotypes (see also Fig. 2E). We observed both small SILTs that did not contain a prominent B-cell follicle and large SILTs with a dense B-cell follicle that were associated with inflammatory infiltrates (e.g., compare the SILTs designated "a" and "b" in Fig. 2C and D). Accordingly, the presence of B-cell follicles in SILT did not closely correlate with the presence of infiltrates in these structures (e.g., the SILTs designated "c" and "d" in Fig. 2C and D). Despite this finding, the strict physical association of inflammatory foci with SILT suggests that, similar to PP, SILT supports productive *Salmonella* infection.

***Salmonella* efficiently utilizes large SILTs for mucosal infection.** To show that *Salmonella* efficiently uses large SILTs for mucosal infection, we applied anti-*Salmonella* antibody staining in order to detect *Salmonella* in SILT at different time points after infection. Such analysis revealed that in BALB/c mice *Salmonella* could be detected in roughly 40% of all SILTs at days 2, 5, and 7 postinfection (Fig. 3A and data not shown). At 13 days postinfection, similar to the situation observed in PP, the frequency of *Salmonella*-bearing SILTs dropped, indicating a clearance of bacteria (Fig. 3A). Thus, the percentage of *Salmonella*-bearing SILTs observed 13 days postinfection is not representative for the frequency of SILTs originally infected. Even though the frequency of *Salmonella*-bearing SILTs was generally lower in C57BL/6 mice, salmonellae could be detected in $17\% \pm 8\%$ of all SILTs at day 7 postinfection ($n = 4$ mice, 138 SILTs were analyzed), demonstrating that in both strains SILT constitutes a site of *Salmonella* infection.

In order to delineate the molecular requirements of *Salmonella* to infect SILT, *Salmonella* strains carrying mutations in either *sipB* or *ssrB*, in addition to *aroA*, were used (see Materials and Methods). Mutation of *sipB* functionally disrupts the type 3 secretion system encoded by *Salmonella* pathogenicity island 1 (SPI-1), whereas a mutation of *ssrB* inactivates the

section were automatically assembled. PP infiltrated by $GR\text{-}1^+$ cells are designated PP, lymphoid aggregations devoid of GR-1-expressing infiltrating cells are indicated by white arrows, and lymphoid aggregation infiltrated by $GR\text{-}1^+$ cells are indicated by red arrows. The boxed area is shown in a magnification in the inset image in panel A. (B) Horizontal sections through the intestinal wall were stained, analyzed, and annotated as described for panel A. Magnifications of the boxed regions illustrating two infiltrated lymphoid aggregations (a and b) and two structures that do not shown signs of inflammation (c and d) are shown in panel C. Nuclei are white, $GR1^+$ cells are red, and $CD11b^+$ cells are green. Double-positive cells expressing GR-1 and CD11b appear yellow. (D) On serial sections the area corresponding to the boxed regions was analyzed for $CD11c^+$ dendritic cells (green) and $B220^+$ B cells (red). (E) Schematic illustration of SILT as seen in vertical and horizontal sections. $B220^+$ B cells, $cKit^+$ cells, and $CD11c^+$ dendritic cells constitute the major cellular components of such aggregates and localize in typical patterns. Small structures dominated by $cKit^+$ cells are also designated CP. CP can develop into ILF in which a distinct B-cell follicle is predominant. However, the majority of all lymphoid structures display intermediate phenotypes that represent transitional phenotypes between CP and ILF. The entire spectrum of small lymphoid aggregation is referred to as SILT encompassing CP, ILF, and structures of intermediate phenotypes. Scale bars: 2 mm in panels A and B and 100 μm in panels C and D.

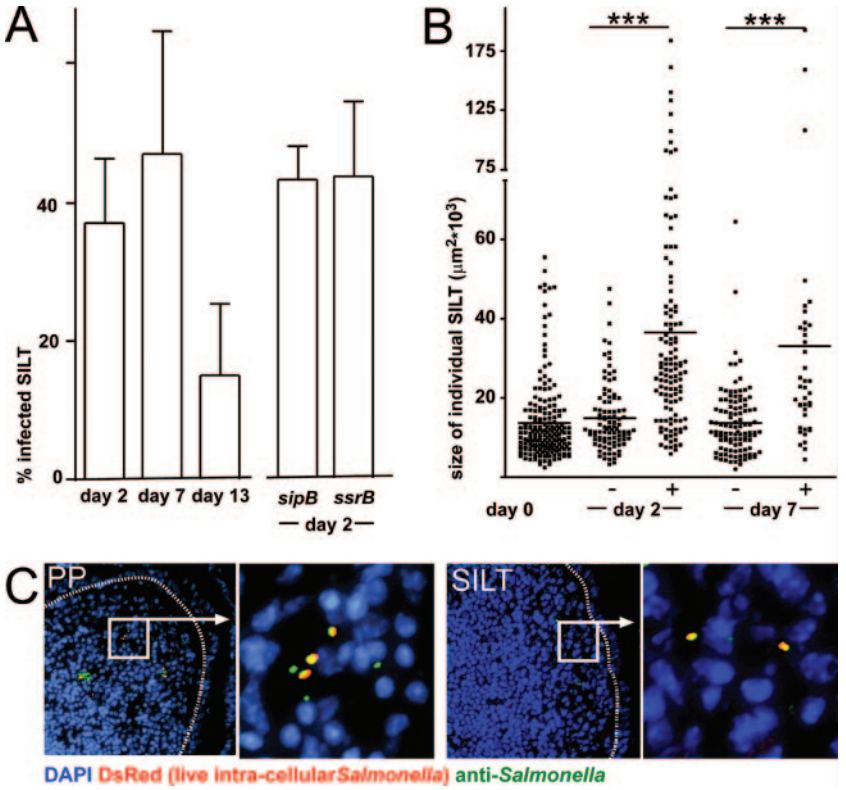

FIG. 3. The presence of *Salmonella* in SILT was analyzed by immunofluorescence microscopy. (A) The percentage of infected SILT was determined by anti-*Salmonella* antibody staining at days 2, 7, and 13 postinfection in BALB/c mice. In addition, the percentage of infected SILTs was determined 2 days after infection by SL1344 *aroA sipB* and SL1344 *aroA ssrB* double-deficient *Salmonella* strains. Columns and error bars depict the means and standard deviations of the fraction of *Salmonella*-positive SILTs observed in individual mice. (B) The sizes of *Salmonella*-positive (+) and negative (−) SILTs before (day 0) and after *Salmonella* infection (day 2 and day 7) are displayed. Dots depict individual SILTs, and horizontal bars depict the mean. *Salmonella*-positive SILTs were significantly larger than *Salmonella*-negative SILTs. ***, $P < 0.001$. (C) Representative fluorescence microscopy images illustrating the presence of *Salmonella* in PP and SILT at 7 days after infection. The nuclei have been stained with DAPI (blue). Anti-*Salmonella* antibody staining is indicated in green, and live intracellular *Salmonella* expressing the red fluorescent protein DsRed are shown in red. Note that all salmonellae expressing the DsRed protein are detected by anti-*Salmonella* antibody staining and thus appear yellow. The dashed line delineates the follicle associated epithelium. Boxed areas are shown at a higher magnification as indicated.

secretion system encoded by SPI-2. We observed, in line with published observations, that 2 days after oral infection both of these *Salmonella* mutant strains were reduced in number in PP compared to the parental strain expressing intact SPI-1 and SPI-2 genes (data not shown). However, the capacity of both mutant strains to infect SILT was comparable to the parental strain. These observations argue that infection of SILT in a high-dose infection model does not essentially depend on these SPI-1- or SPI-2-encoded factors (Fig. 3A).

Subsequently, we compared the sizes of infected and uninfected individual SILTs 2 and 7 days postinfection. SILTs were scored on consecutive vertical sections along the crypt villus axis for the presence of *Salmonella* by antibody staining, and the sizes of all individual SILTs were measured at their maximum dilatation as the SILT area given in square micrometers. At both time points infected SILTs were on average significantly larger than uninfected SILT in BALB/c (Fig. 3B) and C57BL/6 (data not shown) mice. Furthermore, we noted that the size spectrum of infected SILTs encompassed structures occupying more than 60,000 μm^2 in the section area, an order of magnitude which we had never observed in uninfected mice, suggesting that SILTs increase in size as a result of infection. Despite this observation, salmonellae could also be detected in some small SILTs that did not contain a distinct B-cell follicle (Fig. 2B and 3B). No major difference could be detected between the sizes of infected SILTs at days 2 and 7 postinfection. Thus, the increase in SILT size occurs before there is a significant influx of inflammatory cells into infected structures, indicating that additional factors contribute to the overall phenomenon.

Anti-*Salmonella* antibody staining reliably identified *Salmonella* in virtually all SILTs that showed signs of inflammation as judged by the presence of GR-1^+ cells in these structures (data not shown). Conversely, very few uninflamed GR-1^- SILTs displayed anti-*Salmonella* antibody-positive signals, and such signals were virtually absent in uninfected intestines (data not shown). In order to extend our analysis of salmonellae present in intestinal tissues to the normal mucosa, we used a *Salmonella* mutant expressing the red fluorescent protein DsRed (see Materials and Methods). This method only detects live intracellular bacteria and thus provides a more restrictive tool that avoids even the low level of nonspecific signals obtained by

antibody staining. Importantly, all live *Salmonella* strains identified by their red fluorescence also stained with the anti-*Salmonella* antibody, whereas only a fraction of all *Salmonella* strains identified by the antibody also showed a red fluorescent DsRed signal (Fig. 3C). Corroborating our results obtained by antibody staining (Fig. 3A), red fluorescent *Salmonella* strains were readily detectable in both PP and SILT 2 and 7 days after infection.

In evaluating more than 250 cryosections of intestinal rolls obtained from 10 individual infected mice, we detected a total of 13 single red fluorescent salmonellae inside normal villi (data not shown). In each of these sections roughly 4 cm of intestinal tissue was examined. Based on a section thickness of 8 μm and a circumference of roughly 8 mm for the intestinal tubes, we estimated that the 250 sections examined are equivalent to a complete set of serial sections through a 10-cm-long fragment of the murine intestine. This indicates that in the entire small intestines of *Salmonella*-infected mice fewer than 50 live intracellular salmonellae are present in the non-PP non-SILT mucosa. In contrast, we detected a total of 460 SILTs in this set of sections, which allows estimating that 1,000 to 1,500 SILTs are present in the entire small intestine, which is in good agreement with previous observations (24). This indicates that the number of salmonellae present in SILT is much higher than in normal villi. This demonstrates that, although salmonellae might enter intestinal tissue outside the PP and the SILT, this process is very inefficient compared to salmonellae entering the PP and SILT.

In order to link the presence of *Salmonella* in SILT in the early stages of infection with the appearance of inflammatory sites at late stages of infection, the next step was to determine the frequency of SILTs in the small intestine of infected and uninfected mice. We found, in agreement with our previously reported observations, that in uninfected BALB/c mice SILTs are present at a frequency of 42 ± 6 SILTs/cm^2 of intestinal wall. This frequency of SILTs remained unchanged in *Salmonella*-infected mice (Fig. 4A), demonstrating that *Salmonella* infection neither induces the de novo formation of SILT nor diminishes its presence significantly. However, we noted a nonsignificant trend toward less SILT at day 13 postinfection, which might result from severe tissue destruction of infected SILT, thereby complicating proper assessment of these structures. We finally determined the frequency of GR1$^+$ inflammatory foci using horizontal sections. Counting the number of inflammatory foci and measuring the total area analyzed, we estimated that at day 13 postinfection such foci occur at a mean frequency of 18 ± 6 foci/cm^2 of the intestinal wall in BALB/c mice (n = 8, 1 to 3 cm^2 of the intestinal wall was analyzed for each animal). Collectively, a total of several hundred inflammatory foci are present in the entire intestinal mucosa of *Salmonella*-infected mice outside the PP. Notably, the percentage of infected SILTs determined early after infection by anti-*Salmonella* antibody staining (40% of all SILTs bear *Salmonella* by 2 days postinfection, Fig. 3A) and the frequency of SILTs (42 SILTs/cm^2 of intestinal wall, Fig. 4A) allowed us to estimate that *Salmonella* invasion of SILT occurs at a frequency of 18 foci/cm^2, thereby strikingly matching the number of inflammatory sites observed during late stages of infection (13 days postinfection, Fig. 4B).

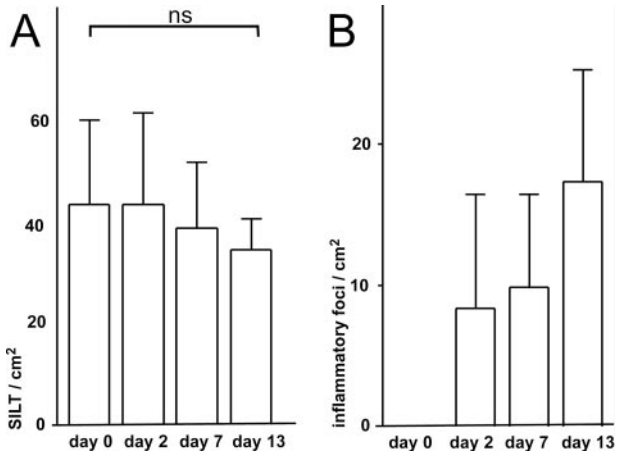

FIG. 4. *Salmonella* infection does not affect the frequency of SILTs but results in the appearance of inflammatory foci in the intestinal mucosa. Before and 2, 7, and 13 days after *Salmonella* infection the frequency of SILTs (A) and the frequency of GR1$^+$ inflammatory foci (B) were determined by immunofluorescence microscopy of horizontal sections through the crypt zone. Bars and error bars depict the means and standard deviations of ≥4 mice analyzed. ns, not significant.

DISCUSSION

Many enteropathogens are able to actively invade host tissues, where they proliferate locally and/or disseminate to distant body sites (4). It is well known that in susceptible mouse strains *S. enterica* serovar Typhimurium can penetrate the intestinal barrier and colonize the spleen and liver, resulting in a typhoid fever-like lethal disease (30). Important virulence determinants of *Salmonella* are encoded by two major chromosomal regions known as SPI-1 and SPI-2 (6, 22), mediating predominantly the uptake of bacteria and intracellular propagation, respectively. In particular, the type 3 secretion system encoded by SPI-1 genes facilitates the entry of *Salmonella* via M cells and contributes to its invasiveness (13). Invasion of PP by *Salmonella* results in a massive inflammatory response, including the recruitment of neutrophils and macrophages into the infected organ. However, several PP-independent mechanisms of *Salmonella* entry into the host have been suggested, most importantly via M cells in the FAE of isolated lymphoid follicles, by intravillus M cells, by lamina propria dendritic cells, and via uptake by enterocytes (see above). Notably, despite the evidence that these mechanisms are able to support *Salmonella* uptake into mucosal tissue the biological significance of these mechanisms has not yet been evaluated.

In the present study we investigated the concept that productive infection of host tissue would manifest itself by local inflammation at the sites of primary invasion. We observed, in line with this idea, that *Salmonella* is present in all PP at 2 days postinfection and that in all PP an ensuing inflammatory response occurs. Consequently, additional sites of *Salmonella* invasion might also induce a local inflammation. Indeed, we observed numerous inflammatory foci in the intestinal mucosa outside PP in infected mice but not in uninfected mice. Since such foci are found scattered throughout the intestinal wall in a pattern independent of PP localization, this finding clearly indicates that *Salmonella* entry into the tissue does not strictly depend on the PP. A detailed analysis of these inflammatory

sites revealed that such foci are infiltrated SILTs, as judged by morphological criteria and antibody immunostaining of all major cellular constituents of SILT. SILT constitutes a heterogeneous spectrum of lymphoid aggregations that frequently possess M cells that might mediate invasion by *Salmonella*.

Salmonella could be detected 2 days after infection in roughly 40% of all SILTs in BALB/c mice. Strikingly, in BALB/c mice the number of *Salmonella*-positive SILTs observed at day 2 postinfection matches the number of inflammatory foci at 7 and 13 days postinfection, suggesting that all infected SILTs develop immunopathology. Similarly, a lower frequency of *Salmonella*-bearing SILTs in C57BL/6 mice correlates with a lower frequency of inflammatory foci in these mice (data not shown), further emphasizing that local influx of inflammatory cells is a general hallmark of productive *Salmonella* invasion. Importantly, such a view would exclude that the overall number of initial sites of *Salmonella* invasion would considerably exceed the number of inflammatory foci observed later during infection. In line with this, we observed that live DsRed-expressing salmonellae were readily identified in PP and SILT but extremely rare outside organized lymphoid tissues. Thus, the uptake of bacteria via intravillus M cells (12) and lamina propria dendritic cells (21) might represent a rare event. In line with this observation, direct evidence for efficient pathogen uptake by lamina propria dendritic cells has not been provided thus far and might be restricted to the terminal ileum in some mouse strains (17, 33). Interestingly, targeting of SILT by *Salmonella* did not depend on functional SPI-1- or SPI-2-encoded type 3 secretion systems. This supports the idea that infection of SILT by *Salmonella* is an M-cell-mediated event and might not strictly depend on *Salmonella*-expressed virulence factors. M cells are specialized cells that transport particulate antigens including pathogens but also innocuous particles such as latex beads from the gut lumen into the PP and SILT (19, 31). Thus, although SPI-1 facilitates M-cell targeting it is not essential for *Salmonella* targeting PP and SILT.

Although it is evident that systemic dissemination of enteropathogens does not strictly depend on their ability to colonize local lymphoid tissue at their site of entry (2, 3, 9), we demonstrate here that local mucosal inflammation is mostly restricted to M-cell-containing structures, i.e., PP and SILT. Notably, the presence of SILT is a general feature of many species, including mice, rats, and humans (24), and in human typhoid fever inflammation it is observed in PP and solitary lymphoid follicles (15). This suggests that the prominent role of SILT during *Salmonella* infection described here is not restricted to the mouse model.

Uncoupling the processes of *Salmonella*-induced pathogenesis at systemic and mucosal sites allows us to reconcile various studies discussing different mechanisms for the uptake of enteropathogens into mucosal tissues and the apparent lack of protection against fatal systemic bacteremia once such mechanisms are disrupted. This does not rule out after all that local tissue injury caused by mucosal inflammation could propagate subsequent systemic spreading of enteropathogens or more dramatically result in intestinal perforation, one of the most serious complications of severe human typhoid fever (25).

In conclusion, we suggest that in mice SILT and PP support infection by *Salmonella*, resulting in severe immunopathology at both sites. Infection of SILT leads to enlargement of infected structures and to local tissue destruction but does not trigger neogenesis of intestinal lymphoid tissue.

ACKNOWLEDGMENTS

This study was supported by Deutsche Forschungsgemeinschaft grants SFB621-A11 and SFB621-A9 to O.P. and D.B.

We thank A. Misslitz and G. Bernhardt for critically reading the manuscript.

REFERENCES

1. **Andersen, J. B., C. Sternberg, L. K. Poulsen, S. P. Bjorn, M. Givskov, and S. Molin.** 1998. New unstable variants of green fluorescent protein for studies of transient gene expression in bacteria. Appl. Environ. Microbiol. **64:**2240–2246.
2. **Barnes, P. D., M. A. Bergman, J. Mecsas, and R. R. Isberg.** 2006. *Yersinia pseudotuberculosis* disseminates directly from a replicating bacterial pool in the intestine. J. Exp. Med. **203:**1591–1601.
3. **Barthel, M., S. Hapfelmeier, L. Quintanilla-Martinez, M. Kremer, M. Rohde, M. Hogardt, K. Pfeffer, H. Russmann, and W. D. Hardt.** 2003. Pretreatment of mice with streptomycin provides a *Salmonella enterica* serovar Typhimurium colitis model that allows analysis of both pathogen and host. Infect. Immun. **71:**2839–2858.
4. **Cossart, P., and P. J. Sansonetti.** 2004. Bacterial invasion: the paradigms of enteroinvasive pathogens. Science **304:**242–248.
5. **Datsenko, K. A., and B. L. Wanner.** 2000. One-step inactivation of chromosomal genes in *Escherichia coli* K-12 using PCR products. Proc. Natl. Acad. Sci. USA **97:**6640–6645.
6. **Galan, J. E.** 1996. Molecular genetic bases of *Salmonella* entry into host cells. Mol. Microbiol. **20:**263–271.
7. **Grutzkau, A., C. Hanski, H. Hahn, and E. O. Riecken.** 1990. Involvement of M cells in the bacterial invasion of Peyer's patches: a common mechanism shared by *Yersinia enterocolitica* and other enteroinvasive bacteria. Gut **31:** 1011–1015.
8. **Hamada, H., T. Hiroi, Y. Nishiyama, H. Takahashi, Y. Masunaga, S. Hachimura, S. Kaminogawa, H. Takahashi-Iwanaga, T. Iwanaga, H. Kiyono, H. Yamamoto, and H. Ishikawa.** 2002. Identification of multiple isolated lymphoid follicles on the antimesenteric wall of the mouse small intestine. J. Immunol. **168:**57–64.
9. **Handley, S. A., R. D. Newberry, and V. L. Miller.** 2005. *Yersinia enterocolitica* invasin-dependent and invasin-independent mechanisms of systemic dissemination. Infect. Immun. **73:**8453–8455.
10. **Hoiseth, S. K., and B. A. Stocker.** 1981. Aromatic-dependent *Salmonella typhimurium* are non-virulent and effective as live vaccines. Nature **291:**238–239.
11. **Hooper, L. V., and J. I. Gordon.** 2001. Commensal host-bacterial relationships in the gut. Science **292:**1115–1118.
12. **Jang, M. H., M. N. Kweon, K. Iwatani, M. Yamamoto, K. Terahara, C. Sasakawa, T. Suzuki, T. Nochi, Y. Yokota, P. D. Rennert, T. Hiroi, H. Tamagawa, H. Iijima, J. Kunisawa, Y. Yuki, and H. Kiyono.** 2004. Intestinal villous M cells: an antigen entry site in the mucosal epithelium. Proc. Natl. Acad. Sci. USA **101:**6110–6115.
13. **Jones, B. D., and S. Falkow.** 1996. Salmonellosis: host immune responses and bacterial virulence determinants. Annu. Rev. Immunol. **14:**533–561.
14. **Jones, B. D., N. Ghori, and S. Falkow.** 1994. *Salmonella typhimurium* initiates murine infection by penetrating and destroying the specialized epithelial M cells of the Peyer's patches. J. Exp. Med. **180:**15–23.
15. **Kraus, M. D., B. Amatya, and Y. Kimula.** 1999. Histopathology of typhoid enteritis: morphologic and immunophenotypic findings. Mod. Pathol. **12:** 949–955.
16. **Lorenz, R. G., and R. D. Newberry.** 2004. Isolated lymphoid follicles can function as sites for induction of mucosal immune responses. Ann. N. Y. Acad. Sci. **1029:**44–57.
17. **Milling, S. W., L. Cousins, and G. G. MacPherson.** 2005. How do DCs interact with intestinal antigens? Trends Immunol. **26:**349–352.
18. **Moghaddami, M., A. Cummins, and G. Mayrhofer.** 1998. Lymphocyte-filled villi: comparison with other lymphoid aggregations in the mucosa of the human small intestine. Gastroenterology **115:**1414–1425.
19. **Neutra, M. R., N. J. Mantis, and J. P. Kraehenbuhl.** 2001. Collaboration of epithelial cells with organized mucosal lymphoid tissues. Nat. Immunol. **2:**1004–1009.
20. **Niedergang, F., and M. N. Kweon.** 2005. New trends in antigen uptake in the gut mucosa. Trends Microbiol. **13:**485–490.
21. **Niess, J. H., S. Brand, X. Gu, L. Landsman, S. Jung, B. A. McCormick, J. M. Vyas, M. Boes, H. L. Ploegh, J. G. Fox, D. R. Littman, and H. C. Reinecker.** 2005. CX3CR1-mediated dendritic cell access to the intestinal lumen and bacterial clearance. Science **307:**254–258.
22. **Ochman, H., F. C. Soncini, F. Solomon, and E. A. Groisman.** 1996. Identification of a pathogenicity island required for *Salmonella* survival in host cells. Proc. Natl. Acad. Sci. USA **93:**7800–7804.

23. **Pabst, O., H. Herbrand, M. Friedrichsen, S. Velaga, M. Dorsch, G. Berhardt, T. Worbs, A. J. Macpherson, and R. Forster.** 2006. Adaptation of solitary intestinal lymphoid tissue in response to microbiota and chemokine receptor CCR7 signaling. J. Immunol. **177:**6824–6832.
24. **Pabst, O., H. Herbrand, T. Worbs, M. Friedrichsen, S. Yan, M. W. Hoffmann, H. Korner, G. Bernhardt, R. Pabst, and R. Forster.** 2005. Cryptopatches and isolated lymphoid follicles: dynamic lymphoid tissues dispensable for the generation of intraepithelial lymphocytes. Eur. J. Immunol. **35:**98–107.
25. **Parry, C. M., T. T. Hien, G. Dougan, N. J. White, and J. J. Farrar.** 2002. Typhoid fever. N. Engl. J. Med. **347:**1770–1782.
26. **Perdomo, O. J., J. M. Cavaillon, M. Huerre, H. Ohayon, P. Gounon, and P. J. Sansonetti.** 1994. Acute inflammation causes epithelial invasion and mucosal destruction in experimental shigellosis. J. Exp. Med. **180:**1307–1319.
27. **Rescigno, M.** 2003. Identification of a new mechanism for bacterial uptake at mucosal surfaces, which is mediated by dendritic cells. Pathol. Biol. **51:**69–70.
28. **Rescigno, M., M. Urbano, B. Valzasina, M. Francolini, G. Rotta, R. Bonasio, F. Granucci, J. P. Kraehenbuhl, and P. Ricciardi-Castagnoli.** 2001. Dendritic cells express tight junction proteins and penetrate gut epithelial monolayers to sample bacteria. Nat. Immunol. **2:**361–367.
29. **Santos, R. L., and A. J. Baumler.** 2004. Cell tropism of *Salmonella enterica*. Int. J. Med. Microbiol. **294:**225–233.
30. **Santos, R. L., S. Zhang, R. M. Tsolis, R. A. Kingsley, L. G. Adams, and A. J. Baumler.** 2001. Animal models of *Salmonella* infections: enteritis versus typhoid fever. Microbes Infect. **3:**1335–1344.
31. **Shreedhar, V. K., B. L. Kelsall, and M. R. Neutra.** 2003. Cholera toxin induces migration of dendritic cells from the subepithelial dome region to T- and B-cell areas of Peyer's patches. Infect. Immun. **71:**504–509.
32. **Sorensen, M., C. Lippuner, T. Kaiser, A. Misslitz, T. Aebischer, and D. Bumann.** 2003. Rapidly maturing red fluorescent protein variants with strongly enhanced brightness in bacteria. FEBS Lett. **552:**110–114.
33. **Vallon-Eberhard, A., L. Landsman, N. Yogev, B. Verrier, and S. Jung.** 2006. Transepithelial pathogen uptake into the small intestinal lamina propria. J. Immunol. **176:**2465–2469.
34. **Vazquez-Torres, A., J. Jones-Carson, A. J. Baumler, S. Falkow, R. Valdivia, W. Brown, M. Le, R. Berggren, W. T. Parks, and F. C. Fang.** 1999. Extraintestinal dissemination of *Salmonella* by CD18-expressing phagocytes. Nature **401:**804–808.
35. **Yamamoto, M., M. N. Kweon, P. D. Rennert, T. Hiroi, K. Fujihashi, J. R. McGhee, and H. Kiyono.** 2004. Role of gut-associated lymphoreticular tissues in antigen-specific intestinal IgA immunity. J. Immunol. **173:**762–769.

Editor: F. C. Fang